RSC Advances

PAPER

View Article Online
View Journal | View Issue

Cite this: *RSC Adv.*, 2018, **8**, 38157

Biosorption of Cr(VI) from aqueous solution using dormant spores of *Aspergillus niger*

Binqiao Ren,[ab] Qiang Zhang,[a] Xiaochen Zhang,[b] Luyang Zhao[b] and Hanyang Li *[a]

Spores of *Aspergillus niger* (denoted as *A. niger*) were used as a novel biosorbent to remove hexavalent chromium from aqueous solution. The effects of biosorbent dosage, pH, contact time, temperature and initial concentration of Cr(VI) on its adsorption removal were examined in batch mode. The Cr(VI) uptake capacity increased with an increase in Cr(VI) concentration until saturation, which was found to be about 97.1 mg g^{-1} at pH 2.0, temperature of 40 °C, adsorbent dose of 2.0 g L^{-1} and initial concentration of 300 mg L^{-1}. Scanning electron microscopy, energy dispersive X-ray spectroscopy, field-emission transmission electron microscopy (FETEM), XPS and Fourier-transform infrared spectroscopy were applied to study the microstructure, composition and chemical bonding states of the biomass adsorbent before and after spore adsorption. The mechanisms of chromate anion removal from aqueous solution by the spores of *A. niger* were proposed, which included adsorption of Cr(VI) onto the spores followed by its reduction to Cr(III). The reduced Cr(III) was rebound to the biomass mainly through complexation mechanisms, redox reaction and electrostatic attraction. The removal of Cr(VI) by spores of *A. niger* followed pseudo-second-order adsorption kinetics. Monolayer adsorption of Cr(VI) was revealed by the better fitting of the Langmuir model isotherm rather than multilayer adsorption for the Freundlich model. The results indicated that *A. niger* spores can be used as a highly efficient biosorbent to remove Cr(VI) from contaminated water.

Received 24th August 2018
Accepted 30th October 2018

DOI: 10.1039/c8ra07084a

rsc.li/rsc-advances

1. Introduction

Chromium contamination (commonly existing as Cr(VI) and Cr(III)) is one of the most important environmental issues, which mainly comes from industry, including the dye and pigment, fertilizer, film and photography, metallurgical, leather and mining industries.[1] Cr(III) and Cr(VI) exhibit very different mobilities and toxicities, with Cr(III) being relatively less soluble and toxic in aqueous systems. In contrast, Cr(VI) is a highly toxic substance with strong solubility, which can induce cancer and mutation.[2] Cr(VI) has been recognized as a serious environmental problem due to its toxicity to living organisms and potential carcinogenicity to humans, thus it has attracted increasing concern for its environmental effects. Due to these differences, the discharge levels of Cr(VI) into surface water is strictly controlled to below 0.05 mg L^{-1} by the U.S. EPA, while total Cr (including Cr(III), Cr(VI) and its other forms) is controlled to below 2 mg L^{-1}.[3] Some physicochemical methods used for the removal of Cr(VI) include chemical reduction and precipitation, solvent extraction, ion exchange, adsorption and membrane separation.[4] However, these methods have limitations, such as secondary pollution, use of expensive equipment and large quantities of chemical reagents, and incomplete metal removal.[5] Thus, alternative biosorption methods are needed.

Metal biosorption is considered to be a more inexpensive and efficient Cr(VI) removal technology due to its simple operation and low energy consumption. Biosorbents that remove heavy metal from wastewater are often classified as algae, microbiological and agricultural waste.[6] The fungal adsorbent in microbial adsorbents can adsorb metal ions efficiently due to the composition of its cell walls (dextran, cellulose, chitin, and protein).[7] Studies on the biosorption of heavy metals on fungi have shown that the fungal cell wall has many functional groups composed of polysaccharides, proteins and lipids, which are responsible for the binding of metals. In the literature on metal biosorption, many studies have been carried out using mycelia of fungal biomass, such as *Mucor*, *Rhizopus* and *A. niger*.[8,9]

Removal of Cr(VI) using *A. niger* fungal biomass has been studied by some researchers.[10,11] Park *et al.* revealed that the removal efficiency of four fungal biosorbents with respect to chromium are as follows: *S. cerevisiae* (44.2%) > *P. chrysogenum* (40.3%) > *A. niger* (29.3%) > *R. oryzae* (23.5%).[12] From their results, *A. niger* fungus has a lower affinity for chromium adsorption than the other two fungi biomass. However, the use of the spores of *A. niger* biomass to improve biosorption capacity has not been investigated to date.

To the best of our knowledge, there has been scarce focus on the removal of metal ions by the spores of *A. niger*. The spores of

[a]*Key Lab of In-fiber Integrated Optics, Ministry Education of China, Harbin Engineering University, Harbin 150080, China. E-mail: hanyang_li@qq.com*
[b]*Institute of Advanced Technology of Heilongjiang Academy of Sciences, Harbin 150080, China*

A. niger have the following advantages over mycelium: (1) small diameter and rough surface; (2) strong survivability; and (3) anti-physical and chemical attack.[13,14] Thus, these characteristics may lead to the feasibility of adsorption of heavy metal ions using *A. niger* spores. The objective of the present study was to investigate the use of spores of *A. niger* as a biosorbent for the removal of Cr(VI) from aqueous solution. The optimum biosorption conditions were determined as a function of dosage of biomass, initial pH, contact time, temperature and initial concentration. The biosorption data was analyzed *via* equilibrium and kinetic studies. The biosorption mechanisms were also investigated *via* SEM-EDS, XPS, FETFM and FTIR analysis.

2. Materials and methods

2.1 Biosorbent preparation

A. niger spores obtained as a reproductive propagule only in solid medium were produced in the late growth stage of *A. niger*.[6] *A. niger* mycelium was acquired from liquid medium.

2.1.1 Preparation of spores of *A. niger*. The *A. niger* strain used in this study was derived from maize straw. The strain was smeared on solid modified Martin medium. *A. niger* spores scattered on the medium were collected, then kept at room temperature for subsequent experiments.

2.1.2 Preparation of *A. niger* mycelium. *A. niger* strain from maize straw was inoculated into liquid Martin medium. After 5 days of incubation, mycelium pellets were harvested and autoclaved for 15 min at 121 °C. Then they were washed with generous amounts of deionized water. After washing, the collected mycelium pellets were dehydrated at 50 °C for 24 h to a constant weight and crushed with a grinder. The dried mycelium powder was stored for further study.[6]

2.2 Chromium solution analysis and uptake capacities

The Cr(VI) stock solution (1000 mg L^{-1}) was prepared by dissolving 2.828 g of $K_2Cr_2O_7$ in 1 L double distilled water. The stock solution was appropriately diluted in distilled water to obtain the experimental solutions of the desired concentration. Inductively coupled plasma mass spectrometry was employed to determine the concentrations of the total Cr before and after biosorption. The amount of Cr(VI) adsorbed by the *A. niger* spores at equilibrium, q (mg g^{-1}), which represents the metal uptake, was evaluated according to the following equation:

$$q = \frac{(C_0 - C_e)}{W} V$$

where, C_0 and C_e are the initial and final concentration of Cr in solution (mg L^{-1}), V is the solution volume and W is the weight of dry spores (g).

2.3 Batch biosorption experiment

In this experiment, the biosorption of Cr(VI) using *A. niger* spores from an aqueous solution was investigated. The optimum conditions (pH, contact time, initial metal ion concentration, temperature and biomass dosage) for the biosorption of Cr(VI) were elucidated. Biosorption experiments were conducted in batch in a 250 mL Erlenmeyer flask with 100 mL metal solution on a rotatory shaker at 120 rpm. After agitation for the desired time, the solutions were centrifuged at 4000 rpm for 5 min and Cr(VI) uptake capacity was calculated based on the supernatant solution.

2.3.1 Effect of dose of sorbent on Cr(VI) sorption. Dosages of *A. niger* spores ranging from 0.05 to 0.25 g, with increments of 0.05 g, were added to 100 mL Cr(VI) solution (100 mg L^{-1}) at pH 2 and their adsorption capacity was calculated. Meanwhile, the *A. niger* mycelium in different dosages, which represents the traditional biosorption method, was compared.

2.3.2 Effect of pH of solution on Cr(VI) sorption. The pH of the solution ranging from 2 to 7, with increments of 1, was maintained at the required value using HCl and NaOH during the study. The experiment was conducted for biosorption at a concentration 100 mg L^{-1} of Cr(VI) and 0.2 g of spores in 100 mL solution.

2.3.3 Effect of contact time on Cr(VI) sorption. The effects of contact time on the biosorption capacity were investigated in the range of 0–300 min. *A. niger* spores (0.2 g) were added to 100 mL of a solution containing 100 mg L^{-1} Cr(VI) in a 250 mL Erlenmeyer flask at pH 2.0.

2.3.4 Effect of initial concentration of solution on Cr(VI) sorption. The effect of initial Cr(VI) concentration was investigated in the range of 25–200 mg L^{-1}. Spore dosage of 0.2 g was added to 100 mL of solution containing varying Cr(VI) concentrations in 250 mL Erlenmeyer flasks at pH 2.0.

2.3.5 Effect of temperature on Cr(VI) sorption. Temperature studies were performed at 20 °C, 30 °C and 40 °C. The spore dosage of 0.2 g was added to 100 mL of Cr(VI) solution with concentrations in the range of 25 to 300 mg L^{-1}.

2.3.6 Effect of other heavy metals on Cr(VI) sorption. Four pairs of competitive biosorption experiments for Cr^{6+} and Na^{+}, Cr^{6+} and K^{+}, Cr^{6+} and Ca^{2+}, and Cr^{6+} and Mg^{2+} ions were performed to investigate the selectivity of the spores for Cr(VI) removal. The initial concentration of all the heavy metals was 100 mg L^{-1}, and the biosorbent dosage was 0.2 g.

2.3.7 Effect of biosorption site on Cr(VI) sorption. The spores were mixed with 40 mL of formaldehyde (HCHO) and 80 mL of formic acid (HCOOH), and the reaction mixture was shaken on a rotary shaker for 8 h at 150 rpm. It has been shown that this treatment results in methylation of the amino groups on the biomass. The spores were suspended in 200 mL of anhydrous methanol, and 2 mL of concentrated hydrochloric acid added to the suspension. The reaction mixture was shaken on a rotary shaker for 8 h at 150 rpm. This treatment was expected to cause esterification of the carboxylic groups present on the biomass.[15]

2.3.8 Effect of real water matrices on Cr(VI) sorption. Songhua River water and groundwater were used as water matrices with 100 mg L^{-1} chromium solution. The spore dosage of 0.2 g was added to 100 mL of Cr(VI) solution in a 250 mL Erlenmeyer flask at pH 2.0.

2.4 Spore characterization

Scanning electron microscopy, energy-dispersive X-ray spectroscopy, field-emission transmission electron microscopy

(FETEM), XPS and Fourier-transform infrared spectroscopy were applied to study the composition, microstructure, chemical status and chemical bonding states of the biomass adsorbent. Scanning electron microscopy (SEM) was used to study the surface morphology before and after spore biosorption. The dried spores were applied to a conductive paste and then sputtered with gold for better image contrast. The image was observed using an SU8010 scanning electron microscope from Japan. FETEM analyses were performed using a Talos F200x field-emission transmission electron microscope from America. In addition, XPS measurements were performed using a PHI 5400 ESCA system equipped with an Al Kα radiation source. Fourier transform infrared spectroscopy (FTIR) analyses were performed using a PerkinElmer instrument to compare the changes in the functional groups before and after spore biosorption.

3. Results and discussion

3.1 The effect of different factors (spore dosage, pH, contact time and initial concentration) on Cr(VI) biosorption

As shown in Fig. 1a, the uptake of the *A. niger* spores was always higher than that of the mycelium at different dosages. When the biosorbent dosage was 0.5 g L^{-1} and the initial concentration was 100 mg L^{-1}, the maximum uptake of the *A. niger* spore biosorbent for Cr(VI) was 58.3 mg g^{-1}, and that for the mycelium was only 12.6 mg g^{-1}. In addition, Table 1 shows some collected data on the biosorption capacity of the pretreated or modified *A. niger* mycelium. The results indicate that the absorption by *A. niger* spores is more advantageous than the traditional mycelium. We also observed a decrease in adsorption capacity with an increase in the dosage of *A. niger* spores. This decrease may be explained as follows: although the total amount of chromium adsorbed by the spores increases, the adsorption capacity per unit of spores is reduced due to the fixed concentration.[18] A similar trend was observed in the mycelium used in this study.

As seen from Fig. 1b, the absorption capacity of *A. niger* spores for Cr(VI) increased with an increase in acidity, reaching a maximum at pH 2. The absorption capacity of Cr(VI) was 1.2 mg g^{-1} at pH 7, which increased to 48.4 mg g^{-1} at pH 2. Other authors have also observed similar results, where the adsorption of Cr(VI) on biomass increased with lowering of pH.[19,20] As the pH decreases, the surface of the spores will be protonated to a higher extent, which results in a stronger attraction towards negatively charged chromate anions such as $HCrO^{4-}$, $Cr_2O_7^{2-}$, CrO_4^{2-}, $Cr_4O_{13}^{2-}$ and $Cr_3O_{10}^{2-}$ in solution. However, as the pH increases, the OH^- ion concentration increases and the total charge on the spore surface becomes negative. This will hinder the biosorption of negatively charged chromate ions, resulting in a dramatic decrease in biosorption capacity at a higher pH.[21] When the pH value is lower than 2, the *A. niger* spores will partially dissolve and their surface chemical nature will change. Therefore, it can be concluded that the adsorption of chromium ions by *A. niger* spores is obviously dependent on the pH of the solution. Electrostatic adsorption plays an important role in this biosorption process.

As can be seen from Fig. 1c, the data collected over 300 min shows that the biosorption of Cr(VI) consisted of two phases: a primary rapid phase and a secondary slow phase. Many studies observed similar results for biosorption by various biomasses.[22,23] The initially rapid phase lasted for about 70 min and the majority of Cr(VI) was absorbed. This suggests that the

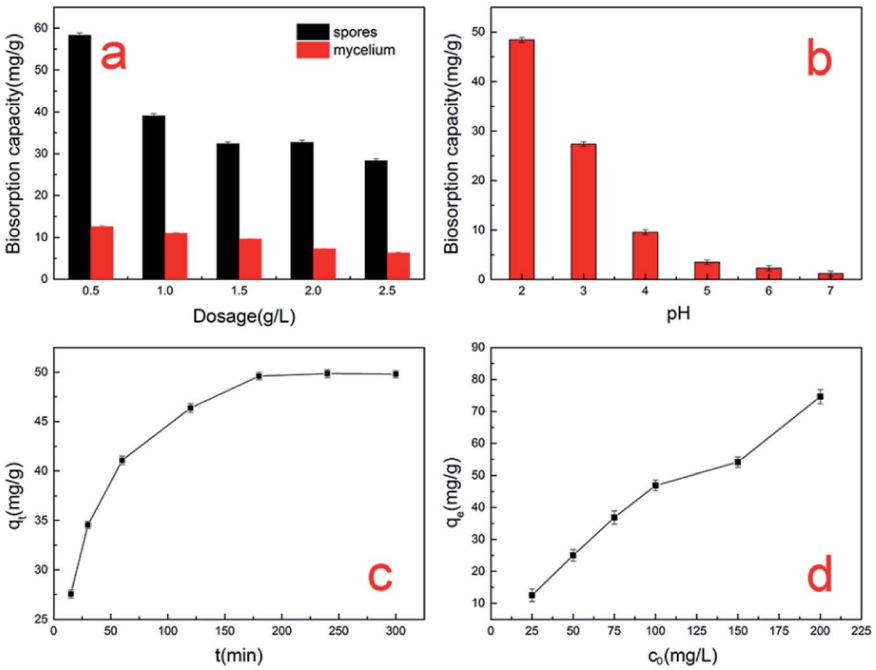

Fig. 1 Effect of factors on the biosorption capacity for Cr(VI) by *A. niger* spores: (a) spore dosage, (b) pH level, (c) contact time and (d) initial concentration.

Table 1 Comparison of the biosorption capacity for Cr^{6+} by spores and mycelium of *Aspergillus niger* under different conditions

Biosorbent	Initial concentration (mg L^{-1})	pH	Biomass dosage (g L^{-1})	Cr^{6+} uptake (mg g^{-1})	Reference
Spores	100	2	0.5	58.3	This study
Mycelium	100	2	0.5	12.6	This study
Autoclaved mycelium	10	2	2	1.5	9
CTAB pretreated mycelium	10	2	2	3.1	9
Acid pretreated mycelium	10	2	2	2.0	9
PEI pretreated mycelium	10	2	2	2.5	9
Dead mycelium	50	2	5	10	16
Mycelium	30	2	4	5.41	17

removal of Cr(VI) was an efficient process. These results were possibly due to electrostatic attraction, extracellular bioreduction, cellular affinity and microprecipitation. After 100 min, the chromium uptake process became relatively slow and reached saturation at about 200 min. This may be due to the reduction of available active sites of spores.[24]

The effect of initial Cr(VI) ion concentration was investigated in the range of 25–200 mg L^{-1}. The results are presented in Fig. 1d. The Cr(VI) biosorption capacity of the spores increased with an increase in the initial concentration of Cr(VI) and then reached the maximum value of about 74.6 mg g^{-1} when the initial concentration was 200 mg L^{-1}. It is worth noting that as the initial concentration increased, the adsorption amount of Cr(VI) increased, which is due to the fact that more active sites on the spore surface were not occupied.[25] From Fig. 1d, we can see that the biosorption capacity rapidly increased in the range of 25–100 mg L^{-1}. The biosorption capacity still increased in the range of 100–200 mg L^{-1}, which indicates the particular suitability of spores for the treatment of effluents at concentrations greater than 200 mg L^{-1}. Thus, we should increase the initial concentration in future studies to determine the maximum initial concentration.

3.2 The effect of temperature on Cr(VI) biosorption

Temperature has been reported to play an important role in biosorption. Therefore, batch experiments were carried out to investigate the temperature dependence of the *A. niger* spores for chromium ion removal. Fig. 2 shows the effect of temperature on the removal of chromium ions at different concentrations. When the concentration was high, an increase in temperature led to a marked increase in the adsorption capacity of the spores. This is mainly due to the sensitivity of the spores themselves to temperature. The Cr(VI) uptake capacity was found to be about 97.1 mg g^{-1} at pH 2.0 at the temperature of 40 °C with an initial concentration of 300 mg L^{-1}.

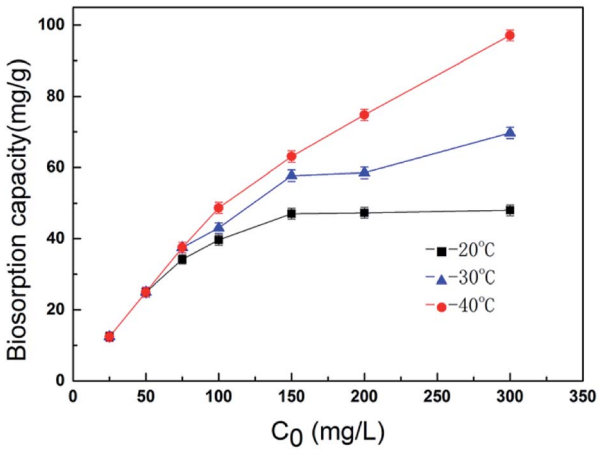

Fig. 2 Effect of temperature on the biosorption capacity for Cr(VI) by *A. niger* spores.

3.3 The effect of other cations on Cr(VI) biosorption

To investigate the selectivity of the spores to remove Cr(VI), other heavy metals such as K^+, Na^+, Ca^{2+} and Mg^{2+} were added separately to the chromium solution. When the biosorbent dosage was 2 g L^{-1} and the initial Cr(VI) concentration was 100 mg L^{-1}, the maximum biosorption value of the spore biosorbent for Cr(VI) was 44.6 mg g^{-1}. When 100 mg L^{-1} ion solutions of K^+, Na^+, Mg^{2+} and Ca^{2+} were added, the biosorption capacity for Cr^{6+} changed from 44.6 mg g^{-1} to 44.24, 46.26, 39.65 and 37.8 mg g^{-1}, respectively (Fig. 3). Thus, ion interference had little influence on the adsorption of Cr(VI) by *A. niger* spores.

3.4 The effect of biosorption site

The functional groups of the spore biomass were modified *via* different chemical treatments to explore the role of different functional groups in the adsorption process.[15] As shown in Fig. 4, the spores masking carboxyl and amino groups showed a significant reduction in adsorption. The adsorption capacity of the unmodified spores was 40.9 mg g^{-1}, which was reduced to 28.2 mg g^{-1} and 7.1 mg g^{-1} when masking the carboxyl and amino groups, respectively. This indicates that amino and carboxyl groups play an important role in the adsorption of chromium ions by *A. niger* spores.

3.5 Effect of real water matrices

To explore the adsorption effect of the *A. niger* spores used in our experiments in the real environment, we designed two sets of controlled experiments. We used Songhua River water and groundwater as the water matrix to explore the adsorption effect of *A. niger* spores. As shown in Fig. 5, the same trend as Fig. 1c was observed, where the adsorption capacity increased rapidly first, and then slowly tended to dynamically balance. Compared to double distilled water as the water matrix, the overall decrease in the adsorption capacity of groundwater and surface

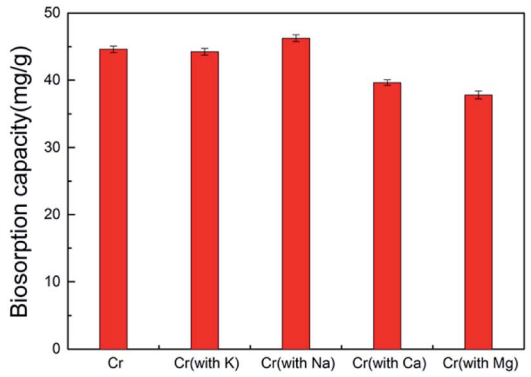

Fig. 3 Biosorption capacity for Cr(VI) and metal ion mixtures with other heavy metals.

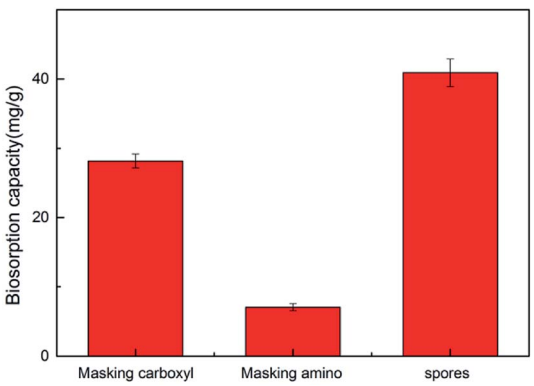

Fig. 4 Amount of metal ions biosorbed by raw biomass and chemically modified biomass.

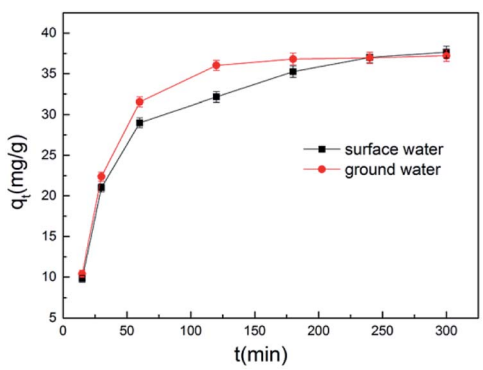

Fig. 5 Biosorption of Cr(VI) using dormant spores of *Aspergillus niger* in aqueous solutions of ground water and surface water.

water as the water matrix may be due to a decrease in the activity of the *A. niger* spores.

3.6 SEM-EDX analysis

Scanning electron microscopy equipped with energy dispersive spectroscopy (SEM-EDX) was used to investigate the changes in the *A. niger* spores as a result of binding with Cr(VI). Fig. 6a and b show the surface morphology of the spores before and after biosorption, respectively. As shown in Fig. 6a, the *A. niger* spores have a small diameter of about 2 μm and some wrinkles on their surface and a spherical and bead-like structure with a high surface/volume ratio. These features provide good conditions for spore adsorption. The SEM image of the *A. niger* spores after biosorption is shown in Fig. 6b, where the wrinkles on the surface of the spores disappear. The SEM image of the spores loaded with Cr obtained at 3 h shows that Cr was distributed on the surface of the *A. niger* spores.

The EDX spectra of the *A. niger* spores before and after the adsorption of Cr(VI) are shown in Fig. 7a and b, respectively. The EDX analysis of the spores after biosorption confirmed the presence of Cr on the surface of the *A. niger* spores with the characteristic EDX peak pattern of Cr in Fig. 7b. According to the EDX results, the chromium content (atomic percentage, at%) on the spore surface (at% of 0 to 7.89) increased, while the C (at% of 80.35 to 76.82) and O (at% of 19.65 to 15.29) contents decreased after Cr(VI) biosorption. There is no doubt that this relative content of C, O and Cr is related to the release of C and O and the adsorption of Cr(VI) on the spore surface during Cr(VI) biosorption, respectively. The O- and C-containing functional groups on the spores possibly contributed to Cr binding on the spores.[26]

3.7 FETEM analysis

FETEM mapping can show the composition and the distribution of elements in the spores. As shown in Fig. 8a, we performed elemental analysis on the micro-domains in the box. Fig. 8b–d show the elements of Cr, C and O on the spores after biosorption, respectively. Cr element was present on the surface of the *A. niger* spores, again indicating that Cr(VI) was adsorbed on the surface of the biomass.

3.8 XPS analysis

XPS was employed to provide the valence state of the chromium bound to the spores. The Cr, O, C, and N peaks can be seen in the low-resolution XPS spectra of the Cr-loaded spores (Fig. 9a). Fig. 9b shows the deconvolution of the high-resolution Cr2p XPS spectrum of the spores. As documented, the characteristic binding energy peaks at 576.8–577.7 and 586.0–588.0 eV correspond to Cr(III), and Cr(VI) contributes a higher binding energy.[27,28] The binding energy peaks in the Cr 2p spectrum were located at 576.95 and 586.45 eV, indicating that the Cr adsorbed on the surface of spores was in the form of Cr(III). No Cr(VI) was detected in the Cr2p XPS spectrum, indicating that the Cr(VI) adsorbed on the adsorbent was completely reduced to Cr(III). Other researches also reached the same conclusion.[16,29,30]

3.9 FTIR analysis

The FTIR spectra of the *A. niger* spores within the wavenumber range of 400–4000 cm^{-1} before and after biosorption were utilized to analyze their functional groups. As shown in Fig. 10, the general profile of the spectra of the spore sample was similar to that of the Cr(VI)-loaded sample, which had adsorbed 100 mg L^{-1} Cr(VI) solution for 3 h. The spores showed strong

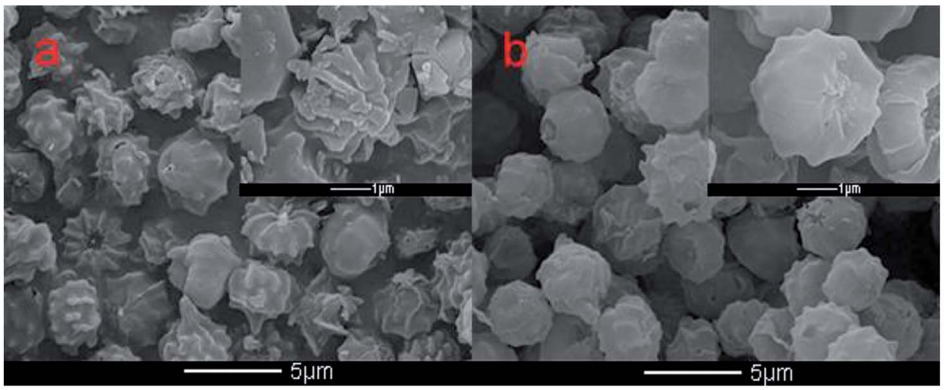

Fig. 6 SEM images of the spores before (a) and after (b) Cr(VI) adsorption.

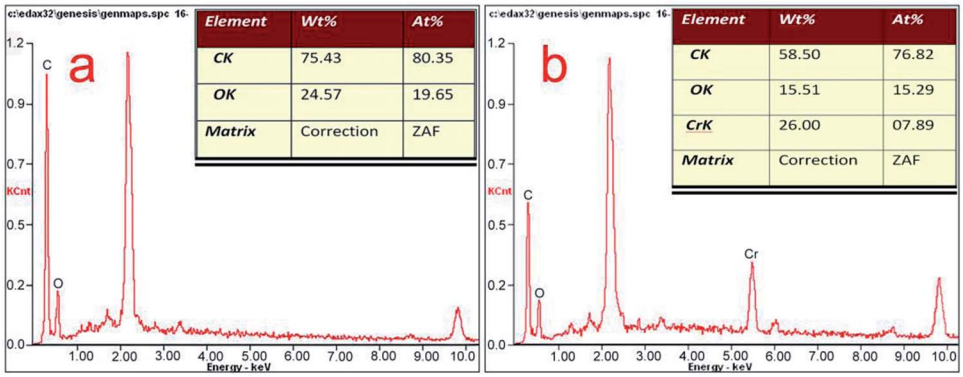

Fig. 7 EDX analysis of the spores before (a) and after (b) Cr(VI) adsorption.

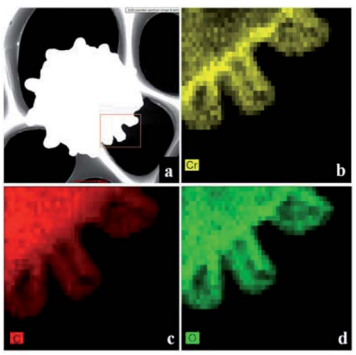

Fig. 8 FETEM images after adsorption by the *A. niger* spores.

peaks at 3448.09, 2925.49, 1648.83., 1558.20, 1382.71, 1081.86, 1033.65 and 582.39 cm^{-1} in the absence of Cr(VI) (Fig. 10a). The figure shows a number of absorption peaks, indicating the complex nature of the examined spores. These peaks are characteristic for bonded hydroxyl groups, CH_2 asymmetric stretch, amide I (protein C=O stretching), amide II (protein N–H bend, C–N stretch), amide III (protein C–N stretch), secondary amide (γ(N–H)+ν(C–N)), pyridine(I)β(C–H) and pyridine(II)β(C–H), respectively.[31–33] It was clear from the comparison of the FTIR spectra of the spores and Cr(VI)-loaded biosorbent that the bonded hydroxyl groups and amide I (protein C=O stretching) shifted visibly from 3448.09 cm^{-1} to 3430.74 cm^{-1} and from 1648.83 cm^{-1} to 1633.41 cm^{-1}, respectively, indicating that these functional groups participated in Cr(VI) binding.

The presence of an CH_2 asymmetric stretching band is mainly due to the lipids, while the existence of amide I, amide II and amide III is largely for proteins, and the pyridine bands are mainly from nucleic acids. The shifts in these functional groups during biosorption show that the proteins and nucleic acids in the biosorbent participated in Cr(VI) binding. The results from FTIR spectroscopy of the spores showed that proteins play an important role as a carrier for Cr(VI) transport and chelating substances. In addition, the appearance of pyridine bands proved that nucleic acids were also the main organics related to biosorption, which also means that the Cr(VI) biosorption was coupled with cellular metabolism and active transport.

3.10 Kinetics analysis

To gain insight into the transport mechanism, kinetics analysis was adopted. The kinetics of the Cr(VI) biosorption was assessed by applying Lagergren's first order kinetic equation and pseudo-second order kinetic equation. As can be seen in Fig. 11, the data analysis showed that the biosorption of Cr(VI) followed the pseudo-second-order kinetic model for all six initial concentrations. This indicates that the adsorption rate of the adsorption process is controlled by chemical sorption.[34] The values of

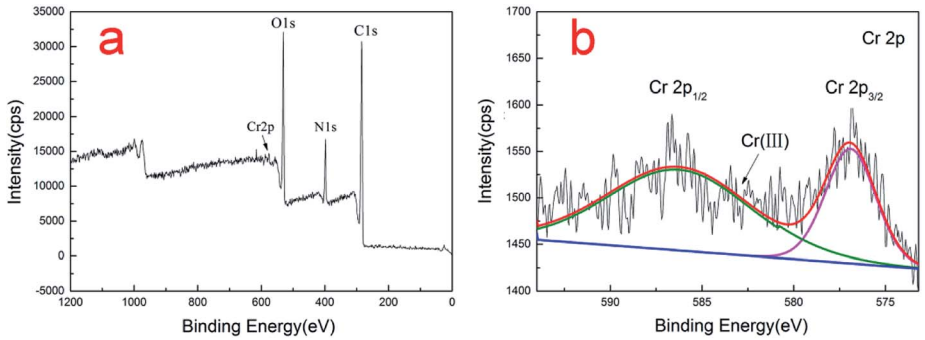

Fig. 9 XPS spectra of (a) spores after Cr(VI) adsorption and (b) Cr 2p1/2 and 2p2/3 orbitals.

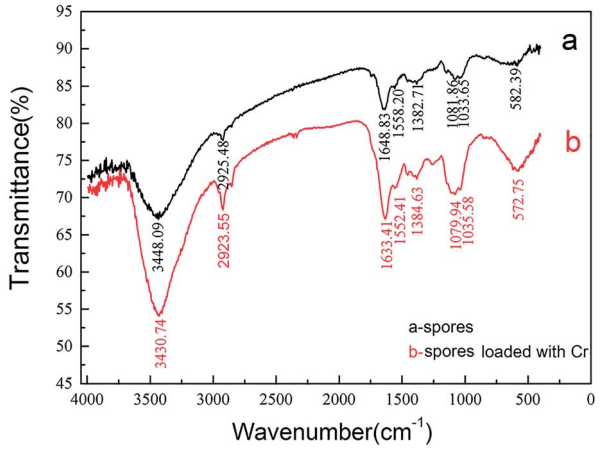

Fig. 10 FTIR spectra of the *A. niger* spores before and after biosorption.

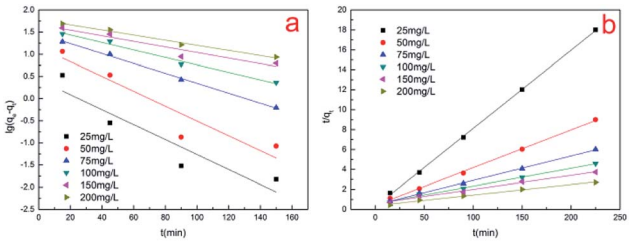

Fig. 11 (a and b) Lagergren's first-order equation and the pseudo-second-order equation, respectively.

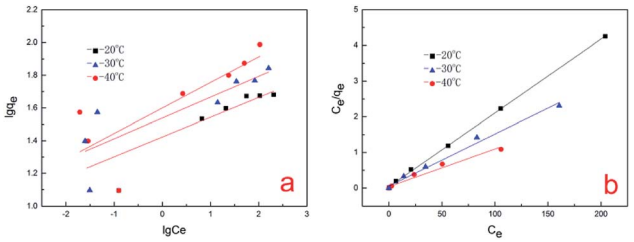

Fig. 12 (a and b) Simulation of Freundlich and Langmuir isotherms, respectively.

various kinetic parameters are given in Table 2. Changing the initial concentration of Cr(VI) affects the kinetic parameters of the adsorption process. As the initial concentration of Cr(VI) increases, the value of the equilibrium absorption capacity (q) increases as expected, but the value of the pseudo-second-order rate constant (k_2) decreases. Compared with the increase in concentration due to saturation of the adsorption sites, the rate of adsorption increases at a slower rate and thus exhibits a decrease in the apparent rate constant (k_2).[5] Other authors have also reported consistent results regarding the kinetics of Cr(VI) adsorption on various adsorbents.[35,36]

3.11 Isotherm analysis

In this study, the Freundlich and Langmuir isotherms models were used to analyze the Cr(VI) sorption data (Fig. 12). The Langmuir isotherm model shows very close agreement with the

Table 2 Simulation of sorption kinetic equations and corresponding parameters

	Lagergren's first-order			Pseudo-second order		
	k_1	q		k_2	q	
C_0 (mg L^{-1})	(min^{-1})	(mg g^{-1})	R^2	(g mg^{-1} min^{-1})	(mg g^{-1})	R^2
25	0.038898	2.66238	0.80714	0.022265	12.75022	0.99945
50	0.038575	14.73941	0.82164	0.003565	26.44803	0.99779
75	0.025794	29.20183	0.9965	0.001309	40.8998	0.99865
100	0.01946	40.2337	0.97945	0.000576	56.14823	0.99385
150	0.014486	46.65734	0.88396	0.00033	71.22507	0.98564
200	0.013265	60.00674	0.98345	0.000291	94.87666	0.9902

Table 3 Simulation of isotherm sorption models and corresponding parameters

	Freundlich			Langmuir		
Temperature (K)	k (L mg^{-1})	n	R^2	b (L mg^{-1})	q_{max} (mg g^{-1})	R^2
293	26.43991	8.246743	0.6625	0.541623	48.33253	0.9995
303	34.58916	7.849294	0.6650	0.26045	68.58711	0.9880
313	39.80797	6.396316	0.5775	0.268888	94.60738	0.9707

experimental adsorption data at temperatures of 20 °C, 30 °C and 40 °C since the R^2 values were 0.9995, 0.9880 and 0.9707, respectively. This indicates that the surface of the *A. niger* spores is homogenous and only one chromium molecule is accepted per active site. The adsorbed molecules are organized into a single layer, and all sites are equal in energy and there is no interaction between the adsorbed molecules.[1] The adsorption parameters for the biosorption of chromium on *A. niger* spores at three temperatures are given in Table 3. The maximum q for Cr(VI) on the *A. niger* spores was increased from 48.33253 to 94.60738 mg g^{-1} with an increase in temperature from 20 °C to 40 °C. Other researchers have reported similar results.[37,38] The increase in spore adsorption capacity with an increase in temperature may be due to the increase in the kinetic energy of adsorbent particles, resulting in increased collision frequency.[39]

4. Conclusion

The spores of *A. niger* act as an effective biosorbent to adsorb cationic heavy metals. Experiments showed that the maximum biosorption capacity of the spores is much higher than *A. niger* mycelium. The Cr(VI) uptake capacity increased with an increase in Cr(VI) concentration until saturation, which was found to be about 97.1 mg g^{-1} at pH 2.0, temperature of 40 °C and adsorbent dose of 2.0 g L^{-1}. The biosorption process followed the pseudo-second order and Langmuir models well, indicating that the adsorption process is mainly controlled by chemical sorption. The mechanism of spores removing chromate anions from water includes adsorption of Cr(VI) onto the spores by electrostatic attraction, and then reduction of Cr(VI) to Cr(III) by complexation mechanism and redox reaction. These results were supported by EDX, FETEM, XPS and FTIR analysis. Thus, it may be concluded that *A. niger* spores exhibit potential for the removal of Cr(VI) in aqueous solution. However, further research is needed to establish the process with specific attention to the regeneration of the sorbent and the recovery of the adsorbed metal.

Conflicts of interest

The authors declared that they have no conflicts of interest to this work. We declare that we do not have any commercial or associative interest that represents a conflict of interest in connection with the work submitted.

Acknowledgements

This work was funded by the National Natural Science Foundation of China (No. 61605031). Science Foundation of Heilongjiang Academy of Sciences (No. ZNBZ2018GJS04). Science Foundation of Department of Science and Technology of Heilongjiang Province (No. YS17A06).

Notes and references

1 Y. Khambhaty, K. Mody, S. Basha and B. Jha, *Chem. Eng. J.*, 2009, **145**, 489–495.
2 J. Barnhart, *Regul. Toxicol. Pharmacol.*, 1997, **26**, S3–S7.
3 A. Baral and R. D. Engelken, *Environ. Sci. Policy*, 2002, **5**, 121–133.
4 S. K. Mehta and J. P. Gaur, *Crit. Rev. Biotechnol.*, 2005, **25**, 113–152.
5 N. Tewari, P. Vasudevan and B. K. Guha, *Biochem. Eng. J.*, 2005, **23**, 185–192.
6 J. Y. Wang and C. W. Cui, *RSC Adv.*, 2017, **7**, 14069–14077.
7 D. Sud, G. Mahajan and M. P. Kaur, *Bioresour. Technol.*, 2008, **99**, 6017–6027.
8 R. S. Bai and T. E. Abraham, *Bioresour. Technol.*, 2001, **79**, 73–81.
9 D. P. Mungasavalli, T. Viraraghavan and Y. C. Jin, *Colloids Surf., A*, 2007, **301**, 214–223.
10 R. S. Bai and T. E. Abraham, *J. Sci. Ind. Res.*, 1998, **57**, 821–824.
11 K. C. Sekhar, S. Subramanian, J. M. Modak and K. A. Natarajan, *Int. J. Miner. Process.*, 1998, **53**, 107–120.
12 D. Park, Y. S. Yun and J. M. Park, *Process Biochem.*, 2005, **40**, 2559–2565.
13 W. R. Bowen, R. W. Lovitt and C. J. Wright, *Colloids Surf., A*, 2000, **173**, 205–210.
14 B. E. Priegnitz, A. Wargenau, U. Brandt, M. Rohde, S. Dietrich, A. Kwade and R. Krull, *Fungal Genet. Biol.*, 2012, **49**, 30–38.
15 A. Kapoor and T. Viraraghavan, *Bioresour. Technol.*, 1997, **61**, 221–227.
16 D. Park, Y. S. Yun, J. H. Jo and J. M. Park, *Water Res.*, 2005, **39**, 533–540.
17 R. Kumar, N. R. Bishnoi, B. K. Garima and K. Bishnoi, *Chem. Eng. J.*, 2008, **135**, 202–208.
18 Z. K. Wang, C. L. Ye, X. Y. Wang and J. Li, *Appl. Surf. Sci.*, 2013, **287**, 232–241.

19 G. Ç. Dönmez, Z. Aksu, A. Öztürk and T. Kutsal, *Process Biochem.*, 1999, **34**, 885–892.
20 R. S. Prakasham, J. S. Merrie, R. Sheela, N. Saswathi and S. V. Ramakrishna, *Environ. Pollut.*, 1999, **104**, 421–427.
21 H. Niu and B. Volesky, *Hydrometallurgy*, 2003, **71**, 209–215.
22 S. Tunali, I. Kiran and T. Akar, *Miner. Eng.*, 2005, **18**, 681–689.
23 Y. Sağ and Y. Aktay, *Biochem. Eng. J.*, 2002, **12**, 143–153.
24 Y. Sağ and Y. Aktay, *Process Biochem.*, 2000, **36**, 157–173.
25 G. Dönmez and Z. Aksu, *Process Biochem.*, 2002, **38**, 751–762.
26 C. Chen, D. H. Wen and J. L. Wang, *Bioresour. Technol.*, 2014, **156**, 380–383.
27 D. Park, Y. S. Yun and J. M. Park, *J. Colloid Interface Sci.*, 2008, **317**, 54–61.
28 H. X. Chen, J. F. Dou and H. B. Xu, *Appl. Surf. Sci.*, 2017, **425**, 728–735.
29 D. Park, Y. S. Yun and J. M. Park, *Environ. Sci. Technol.*, 2004, **38**, 4860–4864.
30 J. L. G. Torresdey, K. J. Tiemann and V. Armendariz, *J. Hazard. Mater.*, 2000, **B80**, 175–188.
31 D. Park, Y. S. Yun, J. H. Jo and J. M. Park, *Chemosphere*, 2005, **60**, 1356–1364.
32 J. M. Tobin, D. G. Cooper and R. J. Neufeld, *Appl. Environ. Microbiol.*, 1984, **47**, 821–824.
33 T. Mathialagan and T. Viraraghavan, *Bioresour. Technol.*, 2009, **100**, 549–558.
34 Y. Ding, D. B. Jing, H. L. Gong, L. B. Zhou and X. S. Yang, *Bioresour. Technol.*, 2012, **114**, 20–25.
35 R. Elangovan, L. Philip and K. Chandraraj, *J. Hazard. Mater.*, 2008, **152**, 100–112.
36 T. Karthikeyan, S. Rajgopal and L. R. Miranda, *J. Hazard. Mater.*, 2005, **B124**, 192–199.
37 Y. Sağ and T. Kutsal, *Process Biochem.*, 2000, **35**, 801–807.
38 V. K. Gupta, A. K. Shrivastava and N. Jain, Pergamon, 2001, vol. 17, pp. 4079–4085.
39 Y. Nuhoglu and E. Oguz, *Process Biochem.*, 2003, **38**, 1627–1631.